Solid−Liquid Equilibria for the CO_2 + R125 and N_2O + R125 Systems: A New Apparatus

Giovanni Di Nicola,*,† Giuliano Giuliani,† Fabio Polonara,† and Roman Stryjek‡

Dipartimento di Energetica, Università Politecnica delle Marche, 60100 Ancona, Italy, and Institute of Physical Chemistry, Polish Academy of Sciences, Warsaw, Poland

A new experimental setup was built for the estimation of the solid−liquid equilibria of alternative refrigerant systems. The system's behavior was measured down to temperatures of 143 K using two binaries (i.e., carbon dioxide + 1,1,1,2,2-pentafluoroethane (CO_2 + R125) and nitrous oxide + 1,1,1,2,2-pentafluoroethane (N_2O + R125)). The setup enabled us to record not only temperature and composition data but also pressure data. The triple points of the pure fluids contained in the mixture were measured to check the reliability of the new apparatus, revealing a good consistency with the literature. The results obtained for the mixtures were interpreted by means of the Schröder equation.

Introduction

Evaluating the solid−liquid equilibria (SLE) and the eutectic composition of a mixture is fundamental for the chemical and petrochemical industry. SLE also play an important role in refrigeration for the estimation of the lowest temperature at which the blend can be used as a refrigerant fluid, in particular for the very low temperature applications (i.e., cascade refrigerating units). The SLE provide useful information for the pipelines design and in the transport of liquid gases in which the formation of solids could lead to safety problems. In addition, SLE provide theoretical information on the real behavior of studied systems at low temperatures in terms of activity coefficients.

The thermophysical properties of the CO_2 + R125 and N_2O + R125 binary systems were recently studied by the same authors with an isochoric apparatus,[1,2] but no information on the SLE of these binary systems are available in the literature. The present study was also undertaken to partially fill this gap.

Most SLE measurements[3,4] enable the visual observation of the disappearance of the last amount of solid phase and a relatively easy temperature control. The experimental temperature ranges usually spans from (200 to 400) K, that is, from (315 to 395) K[3] and from (193 to 280) K.[4] In addition, pressure data are not very frequently acquired during the SLE acquisition.[4] Since the systems under study could be expected to have temperature ranges from 200 K down to about 140 K and system pressures even higher than a few dozen atmospheres throughout the experimental cycle, including sample charging, we decided that it would be technically more feasible to use a method with no visual observation of phase behavior. A setup was specifically built for this purpose. In a recent work,[5] the behavior of the CO_2 + N_2O, CO_2 + R32, and N_2O + R32 binary systems was studied. In this paper, the system's behavior was measured down to temperatures of 143 K for two binaries (i.e., CO_2 + R125 and N_2O + R125).

* Corresponding author. Fax: +39 071 220 4770. E-mail: g.dinicola@univpm.it.
† Università Politecnica delle Marche.
‡ Polish Academy of Sciences.

Description of the Apparatus

Measurement Cell. The experimental setup is shown in Figure 1. The measuring cell (1), with a volume of approximately 47 cm^3, was made out of a stainless steel cylinder with a cover welded to the body. Before welding, a stirrer (3) consisting of a stainless steel rod having a rounded end with two steel blades welded onto it was placed in the cell. The stirrer was kept in a perfectly vertical position by means of conical seats created on the raised bottom of the cell and on the underside of the cover so as to contain the rounded ends of the rod. Two holes were made in the cover, and a stainless steel tube with a diameter of 4 mm was inserted through and welded to the hole on the left for charging the cell with gas, while the hole on the right, which was 6.25 mm in diameter, was used to contain the thermometer (2), the end of which was inserted down to approximately 2.7 cm from the bottom of the cell. This temperature sensor was kept in said position by a suitable stainless steel support screwed onto the hole with a Teflon seal to ensure tightness. The purpose of the stirrer was to prevent any premature stratification of the fluids comprising the various mixtures, while also assuring a greater homogeneity during the liquefaction and crystallization of the mixture. The stirrer inside the cell was turned by a magnet (4), which drives the plate welded onto the lower end of the rod and shaped so as to follow the bottom of the cell as faithfully as possible. The magnet was housed in a seat made of brass (a material particularly suitable for withstanding the inevitable corrosion induced by the very low temperatures characterizing the processes), which was connected to the shaft of an electric engine (5) driving the rotation of the magnet and thus also of the stirrer inside the cell.

Cooling System. It consisted of all the elements in the apparatus designed for the controlled lowering temperature of the cell and globally included four parts:

(1) a coil consisting of copper tube with a diameter of 6 mm and a thickness 1 mm, placed inside a Dewar filled with liquid nitrogen (6), which absorbs heat from the carrier fluid (compressed air) flowing inside it;

(2) a coil with the same structural features as above, wrapped around the measuring cell and removing heat from the cell by

10.1021/je0603067 CCC: $33.50
Published on Web 10/18/2006

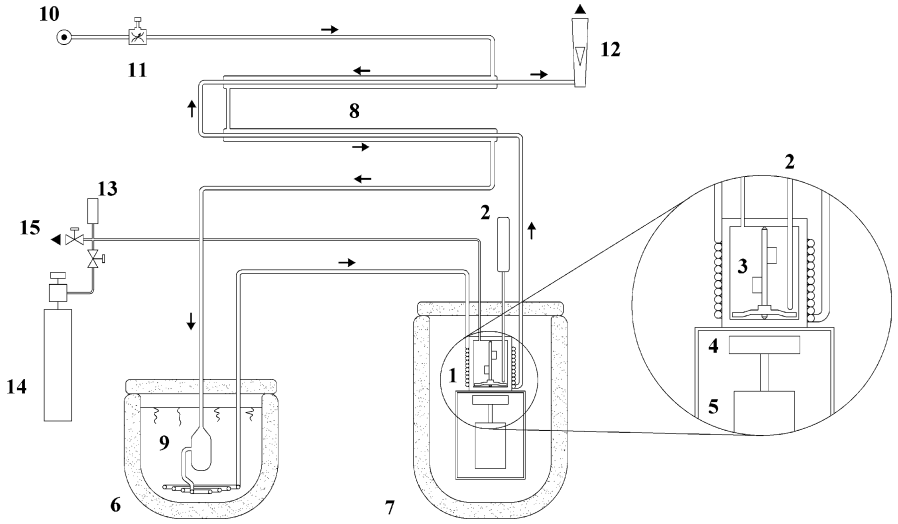

Figure 1. Schematic illustration of the apparatus: 1, measurement cell; 2, platinum resistance thermometer; 3, stirrer; 4, magnet; 5, electric engine; 6, Dewar with liquid nitrogen; 7, Dewar containing the measurement cell; 8, double pipe heat exchanger; 9, ice trap; 10, dry air supplier; 11, mass flow controller; 12, rotameter; 13, pressure trasducer; 14, charging bottle; 15, vacuum pump system.

surface contact due to the cold air circulating inside it. The assembly consisting of the coil and the cell, suitably coated with neoprene (a material with thermal insulation properties), was placed inside a second Dewar (7) so as to increase its thermal isolation;

(3) a double pipe heat exchanger (8). The diameter of the tubes were 6 mm for the inner tube and 16 mm for the outer tube. A flow of air at room temperature entered the exchanger's inner tube, and as it moved through the tube, it was cooled by the backflow heat exchange with the cold air leaving the coil wrapped around the measuring cell. The carrier fluid can thus be precooled, enabling a considerable saving of liquid nitrogen consumption;

(4) an ice trap (9) consisting of a copper base with a diameter of 2.8 mm to ensure the stratification on the inside walls of the ice that forms after the liquefaction and subsequent solidification of the humidity in the carrier fluid circulating in the first coil.

A dry air supplier (10) was installed to overcome any problems relating to air humidity, which would have interfered with its free flow inside the coils, especially at the low temperatures. A mass flow control was installed upstream from the dehumidifier (11): a needle valve with a shutter for adjusting the flow rate, as measured by means of the pressure difference read on a pressure gauge alongside it. The airflow was also measured by a rotameter (12).

Temperature and Pressure Measuring Systems. To monitor the temperatures, the apparatus was equipped with one thermoresistance put in the measuring cell. The system parameters and the efficiency of the regenerative exchanger and of the coil immersed in the liquid nitrogen were assessed using thermocouples at specific points on the copper tube. The platinum resistance thermometer used in the apparatus (100 Ω, Minco, model S7929) was calibrated by comparison with a 25 Ω platinum resistance thermometer (Hart Scientific, model 5680 SN1083).

The pressure values were acquired by an absolute pressure transducer (HBM, model P8A) (13), which can resist up to $1 \cdot 10^4$ kPa, installed in the charging tube. The test pressure readings were taken with the HBM indicator (model MVD 2405). Data are saved by a powered output on the back of the display proportional to the value displayed, which is connected to one of the terminal board inputs. Thus, the data acquisition software enables us to see the trend of the pressure while simultaneously and continuously saving the corresponding values. This transducer was calibrated by connecting the transducer to a dead weight gage.

To obtain the temperature and pressure values, we installed a card (PCI NI 435 by National Instruments) for physical data acquisition. The electric terminals of the sensors are not connected directly to the peripheral but communicate via a SH6868 multipolar cable (National Instruments) with a TBX68T terminal board, where the thermocouples, the thermoresistances, and the digital pressure transducer are physically connected. The information sent to the card is processed by a software developed in LabVIEW 6.1. Temperature and pressure readings were acquired approximately every 2.5 s.

Experimental Procedures and Uncertainties

Given the experimental setup, the measuring cell volume was not separated from the rest of the apparatus. So, the total volume is a sum of the cell volume and of the tube volume. Since the volume of the cell was known from the design data, we also estimated the volume of the tube used to charge it. The aim was to correct the experimental data obtained by estimating the masses of the charged fluids that did not enter the cell, but remained in the rest of the volume.

Experimental Procedure. The charging procedure consisted of the following steps: the bottle containing the refrigerant gas (14) was weighed on the electronic balance (the uncertainty of which is ± 0.5 mg). Then the bottle was connected to the apparatus and to the vacuum pump (15) (Vacuubrand, model RZ2), a vacuum was created inside the measuring cell and the charging tube as recorded on the vacuum pump gauge (Galileo, model OG510). Then the fluid was charged by opening the valve on the gas bottle. The temperature of the cell was brought down by a flow of compressed air cooled with liquid nitrogen so as to insert the whole mass in the cell, leaving as little as possible in the charging tube. A suitable time interval was allowed so that the pressure being lowered by the temperature reduction could drop to below atmospheric pressure. Then the on/off valve was closed. The gas bottle was disconnected and weighed again to establish the actual mass charged in the cell.

During the measurement procedure, the temperature of the sample inside the cell was carefully controlled to fall at uniform rate by the air flowing inside the coil. The air was cooled by

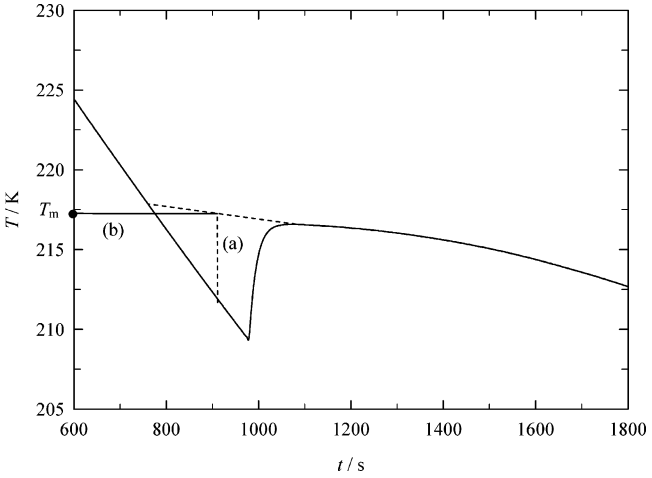

Figure 2. Acquisition of the carbon dioxide triple-point temperature measurements and Rossini method illustration.

putting the coil inside a Dewar filled with liquid nitrogen. The coil was then wrapped around the measuring cell. Monitoring the time dependence of temperature, a cooling curve was obtained for each sample concentration. While the change of phase occurs, the heat removed by cooling is compensated for by the latent heat of the phase change, showing a temperature drop as shown in Figure 2. The arrest in cooling during solidification allows the melting point of the material to be identified on the time−temperature curve. The melting points can then be plotted versus the composition to give a phase diagram.

Uncertainties. The uncertainty on the mass of fluid charged in the measuring cell was calculated using the law of error propagation. In the calculation of the final global uncertainty on the measurement of the mass charged in the cell, we also took into account both the uncertainty of the estimation of the mass in the tube and the uncertainty derived from the difference between the two weights.

In the case of a pure component, for the fluids in question, we considered the uncertainties due to the electronic balance ($\delta m_w = \pm 0.005$ g), the difference between the two weights ($\delta m_1 = \pm 0.007$ g), and the mass trapped in the tube ($\delta m_{cond} = \pm 10$ % $m_{cond} = \pm 0.005$ g), obtaining a total uncertainty for the mass measurement that was less than $\pm$ 0.008 g.

The uncertainty δm_{cond} was obtained as follows:

$$\delta m_{cond} = \pm m_{cond}[(\delta\rho/\rho)^2 + (\delta V/V)^2]^{0.5} = \pm 8.1\ \%\ m_{cond}$$

where $\delta\rho/\rho = 5$ % (estimate of the density ρ from REFPROP 7.0)[6] and $\delta V/V = \pm 6.4$ % (estimate of the volume V). So, as an overestimation, it was set as $\delta m_{cond} = \pm 10$ % m_{cond}.

When the charge was a binary mixture, in order to follow the procedure described herein, all the above considerations were naturally repeated because, in addition to charging a first pure component, we had to charge a second pure component. So the total uncertainty of the mass of sample mixture was less than $\pm$ 0.01 g. As a result, the uncertainty in density, calculated with the law of error propagation, was never greater than $\pm$ 0.05 g·dm.[3] The uncertainty in composition measurements was estimated to be always lower than 0.005 in mole fraction.

The uncertainty of the temperature measurements was assessed on the basis of the uncertainty of the reference instrument, the interpolated standard deviation, and the uncertainty of the measuring system. The uncertainty of the reference instrument was taken to be 0.0016 K, a value obtained from the calibration certificate for the 25 Ω platinum resistance thermometer issued by the G. Colonnetti Metrological Institute in Turin. A standard deviation of $\pm$ 0.019 K was established from the data obtained by the calibration procedure, evaluated with respect to the difference between the temperature calculated (using the interpolating curve equation) and the temperature measured by the sample sensor. The uncertainty of the measuring system was assessed by observing the temperature oscillations around a constant value and was taken to be 0.003 K for the calibrated thermoresistance. The total uncertainty for the thermoresistance, using the law of error propagation, was calculated to be less than $\pm$ 0.023 K.

The uncertainty of the measured pressure was assessed on the basis of the uncertainty of the reference instrument, the interpolated standard deviation of the measurement system's uncertainty, and the uncertainty of the ambient pressure measurement. The uncertainty of the reference instrument (gas lubricated dead weight gage, Ruska, model 2465) amounted to 0.07 % of the measured value. The standard deviation was obtained from the calibration data obtained with respect to the difference between the calculated pressure (using the interpolating curve equation) and the measured absolute pressure (read from the weights on the bench and added to the atmospheric pressure): it amounted to 0.72 kPa. The uncertainty of the measuring system was evaluated, observing the pressure oscillations around a constant value, and was taken to be 2 kPa. The ambient pressure was measured with a vibrating cylinder pressure gauge with an end of scale at 130 absolute kPa and a reported uncertainty of 0.02 % at its end of scale, corresponding to $2.6 \cdot 10^{-2}$ kPa. The global uncertainty of the pressure measurements, considering the single contributions using the law of error propagation, was estimated to be less than $\pm$ 3 kPa.

Results

As concerns the pure fluids, since data are already available in the literature on their triple point, we took the test measurements to confirm these data and thereby verify the functional efficiency and fine adjustment of the apparatus we had designed and constructed. Particular attention was paid to the rate of cooling and the speed of rotation of the stirrer. Regarding the mixtures with constituents considered, there are no data on the SLE in the literature, so the present study covers new ground. The data we obtained can be used as the starting point for future studies.

Chemicals. Carbon dioxide and nitrous oxide were supplied by Sol SpA. Their purity was checked by gas chromatography, using a thermal conductivity detector, and was found to be 99.99 % for both fluids, basing all estimations on an area response. R125 was supplied by Ausimont SpA; its purity was found to be 99.96 % on the basis of an area response.

Pure Fluids. For carbon dioxide, the tests conducted with the stirrer switched off revealed a wider metastable phase than in the tests conducted with the stirrer turning inside the cell: this is probably due to the perturbation induced by the stirrer, which reduces the time margin for the supercooling phase. Even after varying the quantity of CO_2, the supercooling was always greater when solidification occurred with the stirrer switched off. Another feature common to all the experiments was that a faster cooling rate coincided with a greater supercooling effect. The cooling rate that seemed to guarantee the greatest repeatability of the results was approximately -0.01 K·s^{-1}, corresponding to an air flow rate of approximately 0.17 dm^3·s^{-1}. Figure 2 shows an example of a measurement taken for carbon dioxide in which there was evidence of approximately 10 K of supercooling.

Table 1. Temperature and Pressure Triple-Point Measurements for the Pure Fluids

	T	*P*		*T*	*P*		*T*	*P*
fluid	K	kPa	fluid	K	kPa	fluid	K	kPa
CO_2	216.58	524	N_2O	182.02	95	R125	173.10	7
	216.63	509		182.08	96		173.00	4
	216.47	511		181.96	97			
				181.90	79			
avg.	216.56	514	avg.	181.99	92	avg.	173.05	5
lit.	216.59[7,8]	519[8]	lit.	182.34[9,10]	90[9,10]	lit.	172.52[11]	3[12]

Different tests were also conducted for N_2O and R125, using different configurations (with the stirrer on or off). The values obtained with the stirrer on reveal a lesser discrepancy vis-à-vis those reported in the literature, bearing witness to the fact that the homogenizing effect of the stirrer on the temperature of the fluid in the measuring cell has a beneficial influence on the reliability of the test results. Table 1 summarizes the temperatures and pressures recorded at the triple point for the pure fluids and the reference data for these fluids.[7−12] The comparison with the literature data shows a very good agreement in the triple-point measurements for CO_2 and N_2O, while higher discrepancy for R125 with literature[11] was evident. These data relate to the tests conducted with the stirrer switched on.

Results for Mixtures. Measurements were taken using different concentrations of the two components, obtaining a satisfactory number of points, which were then recorded on a concentration/temperature graph ($T-x$). Moreover, after ascertaining the repeatability of the results by performing several tests on different days, for each concentration we evaluated the effect of the stirrer in terms of the miscibility in question and whether the effect of the stirrer could confirm or refute the hypotheses relating to the elimination of the radial temperature gradient, the cancellation of any stratification of the fluids, and a greater homogeneity of the mixture. Conducting several tests on the same sample, we noted that we obtained better, more reliable results by switching off the stirrer before reaching the triple-point temperature. The turning of the stirrer helps to keep the mixture's components or sample well-mixed and the homogeneity of temperature inside the cell. Once near-freezing temperatures have been reached, it probably interferes with the solidification of the mixture. We consequently decided to turn off the stirrer at least about 30 K (a value suggested by experience) beforehand in all the subsequent tests so as to avoid losing the beneficial effect of the stirrer while also avoiding any fragmentation of the solid crystals when they began to form.

The $T-x$ measurements for the two mixtures considered (CO_2 + R125 and N_2O + R125, respectively) are given in Figures 3 and 4 while the $P-x$ measurements are given in Figures 5 and 6 . The results were also summarized in Table 2. From the $T-x$ data, it is evident that both systems form eutectics ($x_1 = 0.14$ at $T = 157$ K for CO_2 + R125 and $x_1 = 0.29$ at $T = 142$ K for N_2O + R125).

Rossini Method Corrections. The results of the temperature data acquisitions were corrected using the Rossini method[13] because a constant cooling rate is not indispensable and was not guaranteed by our experimental method. This is a graphic method that considers the area contained by the tangent to the curve in the descending stretch after the temperature drop and curve itself. Then a vertical segment (a) is taken, which divides the area into two equal parts. Then a second, horizontal segment (b) is obtained from the point of intersection between segment (a) and the tangent to the curve up until it identifies the temperature corresponding to this new point on the axis of the ordinates (T_m). This graphic method is illustrated in Figure 2.

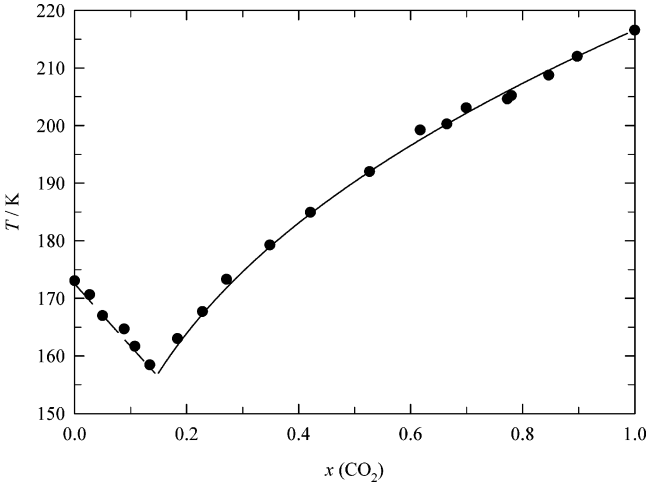

Figure 3. SLE for the CO_2 + R125 system. Black symbols denote the experimental points while the lines denote the Schröder equation.

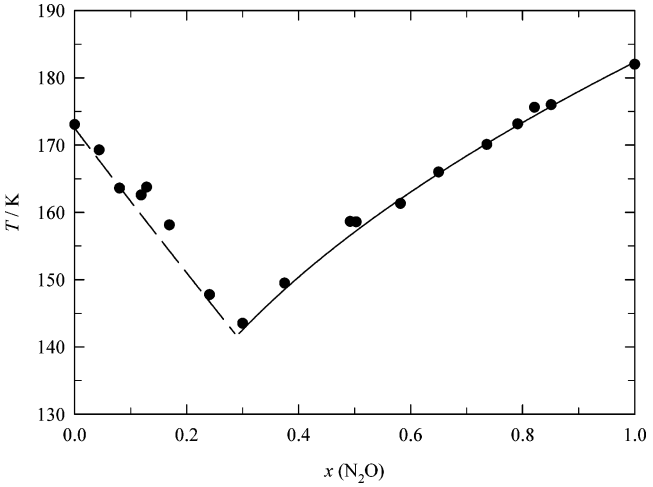

Figure 4. SLE for the N_2O + R125 system. Black symbols denote the experimental points while the lines denote the Schröder equation.

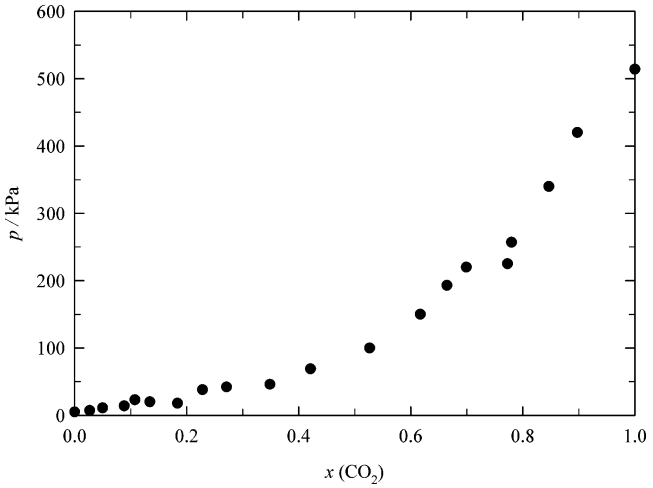

Figure 5. $P-x$ diagram for the CO_2 + R125 system.

The entity of the corrections takes into account the fact that the fluid is still in a liquid state during the metastable state (supercooling) that precedes proper solidification. In this phase, the temperature is distinctly lower than the one characterizing the instant when crystallization begins, its amplitude depending mainly on the rate at which the temperature is lowered. The resulting corrections were nonetheless always very limited, of

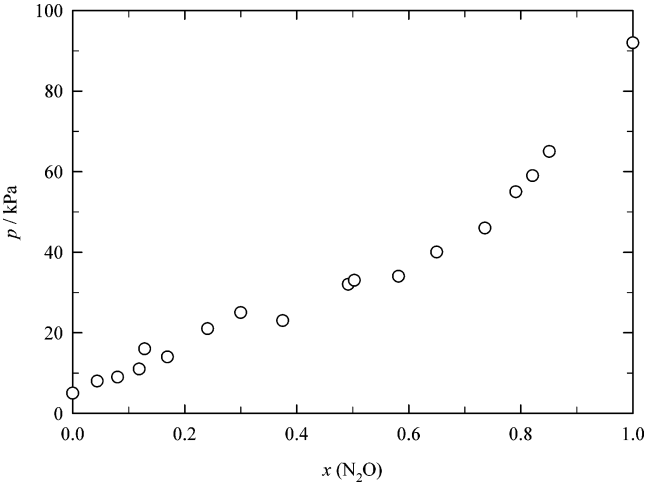

Figure 6. $P-x$ diagram for the N_2O + R125 system.

Table 2. $T-P-x$ Measurements for the CO_2 + R125 and N_2O + R125 Binary Systems

CO_2 (1) + R125 (2)			N_2O (1) + R125 (2)		
x_1	T/K	P/kPa	x_1	T/K	P/kPa
0.000	173.05	5	0.000	173.05	5
0.027	170.64	7	0.044	169.28	8
0.050	167.00	11	0.080	163.60	9
0.088	164.67	14	0.119	162.57	11
0.108	161.67	23	0.129	163.75	16
0.134	158.43	20	0.169	158.12	14
0.184	162.99	18	0.241	147.75	21
0.229	167.68	38	0.300	143.50	25
0.271	173.30	42	0.375	149.47	23
0.349	179.25	46	0.492	158.62	32
0.421	184.95	69	0.503	158.58	33
0.527	192.00	100	0.582	161.30	34
0.617	199.23	150	0.650	166.00	40
0.665	200.25	193	0.736	170.10	52
0.699	203.08	220	0.791	173.13	55
0.773	204.59	225	0.821	175.61	69
0.780	205.22	257	0.851	176.00	75
0.847	208.75	340	1.000	181.99	92
0.897	212.00	420			
1.000	216.56	514			

the order of a few tenths of a Kelvin in the majority of cases, and always well below 1 K.

Interpretation of the Results. The SLE depend both on the crystals formed in solution and on the properties of the liquid phase. Most organic systems form eutectics: in this case, the course of the liquidus is well-described by the Schröder equation, known since the end of the 19th century.[14] The exact course of the liquidus for ideal mixtures (i.e., showing a small deviation from Raoult's law) depends mainly on the property of the solute (CO_2 and N_2O in our case) and, in the case of nonideal systems, on the property of the liquid phase.

As both systems formed eutectics, the solubility of the solid solute in the solvent (here, R125) can be described by the Schröder equation; which disregarding any difference between the heat capacity of the subcooled liquid solute and solid solute takes the following form:

$$\ln \gamma_2 x_2 = -\frac{\Delta h_m}{RT}\left(1 - \frac{T}{T_m}\right) \quad (1)$$

where the subscript 2 denotes the solute and the subscript m denotes property at melting point. Our vapor−liquid assessments[1,2] showed minimal deviations from Raoult's law for all systems, so we assumed as a first approximation that the

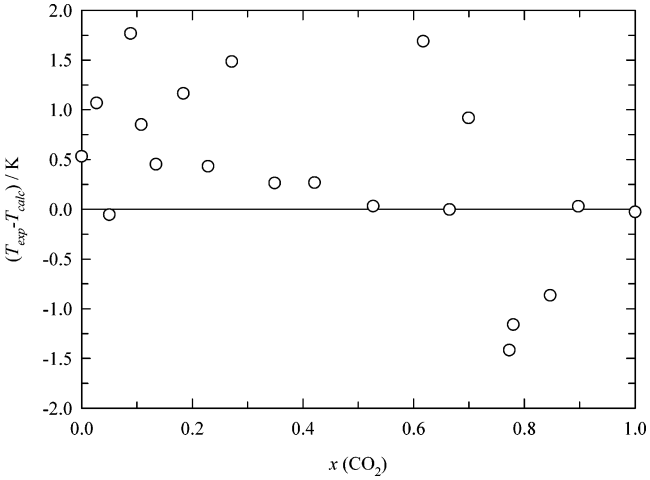

Figure 7. Temperature differences between experimental and calculated data by the Schröder equation for the CO_2 + R125 system.

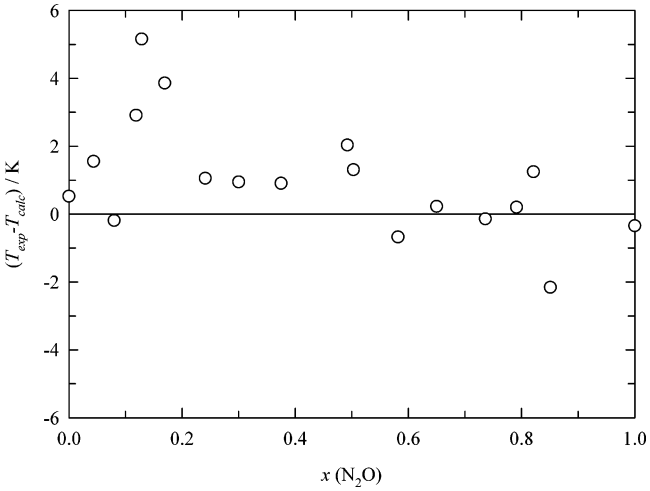

Figure 8. Temperature differences between experimental and calculated data by the Schröder equation for the N_2O + R125 system.

solute's activity coefficient, $\gamma_2 = 1$. This means that we can write

$$\ln x_2 = -\frac{\Delta h_m}{RT}\left(1 - \frac{T}{T_m}\right) \quad (2)$$

This simplification leads to the consideration that the solubility of the solid solute is independent of the solvent as far as the assumptions hold. The enthalpies at melting point (Δh_m) were assumed to be 9020 J·mol^{-1},[15] 6540 J·mol^{-1},[15] and 2249 J·mol^{-1},[11] for CO_2, N_2O, and R125, respectively.

The course of the liquidus calculated with the Schröder equation is included in Figures 3 and 4. The differences between experimental and calculated data by eq 2 temperatures are reported in Figures 7 and 8. Both systems well followed the Schröder equation. For the CO_2 + R125 system, a good agreement with the equation prediction was evident. For the N_2O + R125, a general agreement with the Schröder equation was evident, with higher deviations at lower N_2O concentrations, probably due to increasing difficulties in getting low-temperature data. Considering that our vapor−liquid assessments[1,2] showed minimal deviations from Raoult's law for the systems, the pressure values in the temperature range from (199 to 212) K for the CO_2 + R125 system and from (166 to 176) K for the N_2O + R125 system were compared with Raoult's law prediction extending the metastable state of CO_2 up to 199 K

and for both R125 and N_2O up to 166 K. The comparison showed an AAD of (13 and 15) kPa for CO_2 + R125 and N_2O + R125, respectively.

Conclusion

In this paper, a new experimental setup for the SLE exploration is presented. The SLE behavior of CO_2 + R125 and N_2O + R125 systmes were measured down to temperatures of 145 K. The apparatus enabled us to record not only temperature and composition data but also pressure data. The triple points of the pure fluids contained in the mixture were measured to check the reliability of the new apparatus, revealing a good consistency with the literature. The CO_2 + R125 and N_2O + R125 systems showed the presence of an eutectic and of a good agreement with Schröder equation prediction.

Literature Cited

(1) Di Nicola, G.; Pacetti, M.; Polonara, F.; Stryjek. R. Isochoric measurements for CO_2 + R125 and CO_2 + R32 binary systems. *J. Chem. Eng. Data* **2002**, *47*, 1145−1153.

(2) Di Nicola, G.; Giuliani, G.; Polonara, F.; Stryjek. R. Isochoric *PVTx* measurements for the N_2O + R125 binary system. *J. Chem. Eng. Data* **2006**, *51*, 2041−2044.

(3) Fukné-Kokot, K.; König, A.; Knez, Ž.; Škerget, M. Comparison of different methods for determination of the S-L-G equilibrium curve of a solid component in the presence of a compressed gas. *Fluid Phase Equilib.* **2000**, *173*, 297−310.

(4) Teodorescu, M.; Wilken, M.; Wittig, R.; Gmehling, J. Azeotropic and solid−liquid equilibria data for several binary organic systems containing one acetal compound. *Fluid Phase Equilib.* **2003**, *204*, 267−280.

(5) Di Nicola, G.; Giuliani, G.; Polonara, F.; Stryjek. R. Solid−liquid equilibria in the CO_2 + N_2O, CO_2 + R32, and N_2O + R32 systems. Presented at the 16th Symposium on Thermophysical Properties, July 30−August 4, 2006, Boulder, CO.

(6) Lemmon, E. W.; McLinden, M. O.; Huber, M. L. NIST *Standard Reference Database 23, NIST Thermodynamic Properties of Refrigerants and Refrigerant Mixtures Database (REFPROP)*, Version 7.0; National Institute of Standards and Technology: Gaithersburg, MD, 2002.

(7) Marsh, K. N. *Recommended Reference Materials for the Realization of Physicochemical Properties*; Blackwell Scientific: Oxford, 1987.

(8) Angus, S.; Armstrong, B.; de Reuck, K. M. *International Thermodynamic Tables of the Fluid State—3 Carbon Dioxide*; Pergamon: New York, 1976.

(9) Fonseca, I. M. A.; Lobo, L. Q. Thermodynamics of liquid mixtures of xenon and methyl fluoride. *Fluid Phase Equilib.* **1989**, *47*, 249−263.

(10) Calado, J. C. G.; Rebelo, L. P. N.; Streett, W. B.; Zollweg, J. A. Thermodynamics of liquid (dimethyl ether + xenon). *J. Chem. Thermodyn.* **1986**, *18*, 931−938.

(11) Lüddecke, T. O.; Magee, J. W. Molar heat capacity at constant volume of difluoromethane (R32) and pentafluoroethane (R125) from the triple-point temperature to 345 K at pressures to 35 MPa. *Int. J. Thermophys.* **1996**, *17*, 823−849.

(12) Lemmon, E. W.; Jacobsen, R. T. A new functional form and new fitting techniques for equations of state with application to pentafluoroethane (HFC-125). *J. Phys. Chem. Ref. Data* **2005**, *34*, 69−108.

(13) Mair, B. J.; Glasgow, J. A. R.; Rossini, F. D. Determination of the freezing points and amounts of impurity in hydrocarbons from freezing and melting curves. *J. Res. Natl. Bur. Stand.* **1941**, *26*, 591−620.

(14) Schröder, I. Über die Abhängigkeit der Löslichkeit eines festen Körpers von seiner Schmelztemperatur. *Z. Phys. Chem.* **1893**, *11*, 449−465.

(15) Lide, D. R.; Kehiaian, H. V. *CRC Handbook of Thermophysical and Thermochemical Data*; CRC Press: Boca Raton, FL, 1994.

Received for review July 6, 2006. Accepted September 13, 2006.

JE0603067